Phase diagram of the Holstein-Hubbard two-leg ladder using a functional renormalization-group method

Ka-Ming Tam,[1] S.-W. Tsai,[2] D. K. Campbell,[1] and A. H. Castro Neto[1]
[1]*Department of Physics, Boston University, 590 Commonwealth Avenue, Boston, Massachusetts 02215, USA*
[2]*Department of Physics and Astronomy, University of California, Riverside, California 92507, USA*
(Received 1 May 2007; published 18 May 2007)

Using a functional renormalization-group method, we obtain the phase diagram of the two-leg ladder system within the Holstein-Hubbard model, which includes both electron-electron and electron-phonon interactions. Our renormalization-group technique allows us to analyze the problem for both weak and strong electron-phonon couplings. We show that, in contrast to results from conventional weak-coupling studies, electron-phonon interactions can dominate electron-electron interactions, and retardation effects play an important role on the phase diagram.

DOI: 10.1103/PhysRevB.75.195119 PACS number(s): 71.10.Fd, 71.30.+h, 71.45.Lr, 05.10.Cc

I. INTRODUCTION

The renormalization-group (RG) method has provided a fundamental understanding of the stable phases of matter in terms of the basin of attraction of fixed points (FPs). Quantum phase transitions (QPTs) between different fixed points can be described in terms of the stability of these FPs relative to the RG flow. In the theory of metals, Landau's Fermi-liquid theory can be described either as a stable FP of the renormalization-group flow under repulsive interactions or as an unstable FP under attractive interactions to a superconducting (SC) state described by BCS theory.[1] Apart from determining the stability of a FP, the RG method also provides direct information about the energy scales (gaps) and length scales (correlation lengths) associated with a QPT. Hence, the RG not only provides qualitative information but also quantitative information about the different phases of matter.

In practice, however, there are very few examples of problems in which the RG can be implemented beyond weak coupling.[2] Furthermore, another well-known challenge to the RG has been its implementation in problems with retardation, such as the electron-phonon (e-ph) problem, because of the introduction of multiple, frequency-dependent interaction channels that renormalize in a collective, energy-dependent, way. At weak e-ph coupling, when retardation plays a small role, the RG can be implemented using approximations such as the so-called two-step RG.[3,4] Usually, the two-step RG leads to an enhancement of the instabilities that exist when only electron-electron (e-e) interactions are present, but does not describe phases where retardation effects due to the e-ph coupling become dominant over e-e effects. In fact, we show that new phases, such as charge-density wave (CDW) and *s*-wave SC state, emerge at strong e-ph coupling (see Fig. 1).

Recently, the RG was extended to study the nonperturbative physics of the e-ph problem in the large N limit (where $N=E_F/\Lambda$, E_F is the Fermi energy and Λ is the cutoff) in the presence of e-e interactions for a two-dimensional circular (three-dimensional spherical) Fermi surface.[5] In particular, that work established that the stable FP of this problem is described by the Eliashberg-Migdal theory, which contains BCS as its weak-coupling limit. Since it has few scattering channels,[1] the circular (spherical) Fermi surface, which is a consequence of the plane-wave character of the electronic wave functions, is a particularly simple problem. This is not the case for Fermi surfaces that derive from localized electronic orbitals that can be unstable either to exotic SC states (such as *p* and *d* waves) or to density wave (charge and spin) phases. Arguably, the most famous example of this phenomenon are the one-dimensional (1D) conductors where the nesting associated with Fermi points leads to a richness of phases that can be described by *g*-ology, bosonization,[6,7] and the functional RG.[8] However, the 1D problem is very particular because of the restricted phase space for interaction, and, even in 1D, the treatment of the e-ph interaction is problematic.[9]

The recently developed e-ph coupled functional renormalization group[5] (FRG) includes the merits of the FRG for the pure e-e interacting system[1,10,11] and goes beyond the two-step renormalization group for the e-ph interacting system[3,4,12] by allowing the systematic study of the full frequency dependence of couplings. In this paper, we use this newly extended FRG to study the two-leg ladder Holstein-

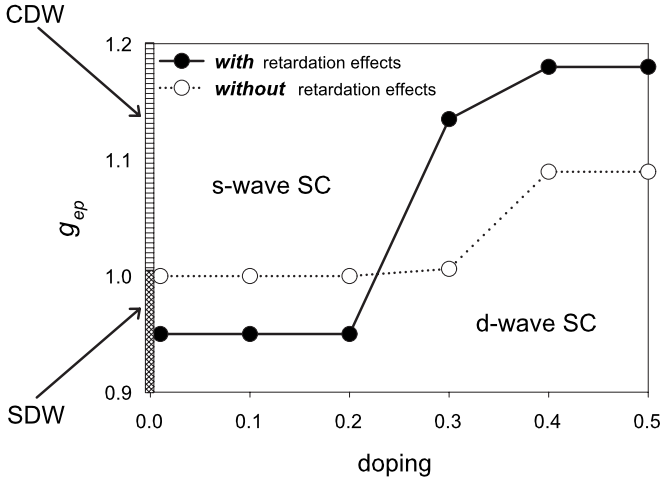

FIG. 1. Phase diagram of Holstein-Hubbard ladder as a function of electron-phonon coupling g_{ep} and doping ($t=1$ and $U=2$). Filled circles, $\omega_0=1$; open circles, without retardation (antiadiabatic limit). Zero doping corresponds to half-filling.

Hubbard model that describes a quasi-1D system in the presence of e-e and e-ph interactions. The ladder system, consisting of two 1D chains coupled by interchain hopping, can be considered as an intermediate between 1D and two-dimensional (2D) systems, since it shares properties with both: it has a limited number of scattering channels, as in 1D, but can also show SC state with 2D characteristics, such as d-wave order parameter.[13,14] As a result, ladders have been considered by many as a theoretical test bed for the understanding of high-T_c superconductivity.[15]

Furthermore, the interest in the e-ph problem in high T_c has been revitalized by experimental evidence that the e-ph coupling may play a critical role in these systems.[16,17] Apart from the cuprates, ladder systems have also attracted much attention recently because, from the technical point of view, they are amenable to field theoretical calculations and to reliable numerical simulations, in contrast to truly 2D systems. Studying the interplay between the e-e and e-ph interactions in a ladder is also important for the understanding of the physics of some low-dimensional materials, such as molecular crystals and charge-transfer solids.[18]

The plan of this paper is to employ this newly developed functional multiscale renormalization-group method to explore the properties of the two-leg ladder with both e-e and e-ph interactions. Thus, Sec. II of the paper, which describes the Holstein-Hubbard model and the allowed scattering terms in the two-leg ladder system, will serve as the basis to illustrate the multiscale nature of the e-ph interacting system. In Sec. III, we present briefly the multiscale functional renormalization-group method. In Sec. IV, we discuss the results, emphasizing the change of the pairing symmetry. Section V contains a brief conclusion.

II. HOLSTEIN-HUBBARD TWO-LEG LADDER

The Holstein-Hubbard model is described by the following Hamiltonian (we use units such that $\hbar=1=k_B$):

$$H = -t\sum_{\langle i,j\rangle,\sigma}(c^{\dagger}_{i,\sigma}c_{j,\sigma}+\text{H.c.}) + U\sum_{i} n_{i,\uparrow}n_{i,\downarrow} + g_{\text{ep}}\sum_{i,\sigma}(a^{\dagger}_{i}+a_i)n_{i,\sigma} + \omega_0\sum_{i} a^{\dagger}_{i}a_i - \mu\sum_{i,\sigma} c^{\dagger}_{i,\sigma}c_{i,\sigma}, \quad (1)$$

where $c^{\dagger}_{i,\sigma}$ ($c_{i,\sigma}$) creates (annihilates) an electron at site i with spin σ ($n_{i\sigma}$ is the electron number operator), $a^{\dagger}_{i}$ (a_i) creates (annihilates) an optical phonon at site i with energy ω_0, t is the hopping energy of the electrons along legs and rungs of the ladder, U is the on-site e-e interaction, g_{ep} is the e-ph coupling energy, and μ is the chemical potential to fix the filling factor. In what follows, we use units such that $t=1$. In the absence of e-e ($U=0$) and e-ph ($g_{\text{ep}}=0$) interactions, the energy spectrum of the electrons is given by

$$\epsilon(k \equiv \{k_x,k_y\}) = -2t\cos(k_x) - t\cos(k_y) - \mu. \quad (2)$$

It has the form shown in Fig. 2.

One can reformulate the problem in terms of path integrals, and since the phonon fields enter quadratically in the action, they can be integrated out exactly,[5] generating an effective action S for the electrons that can be written as

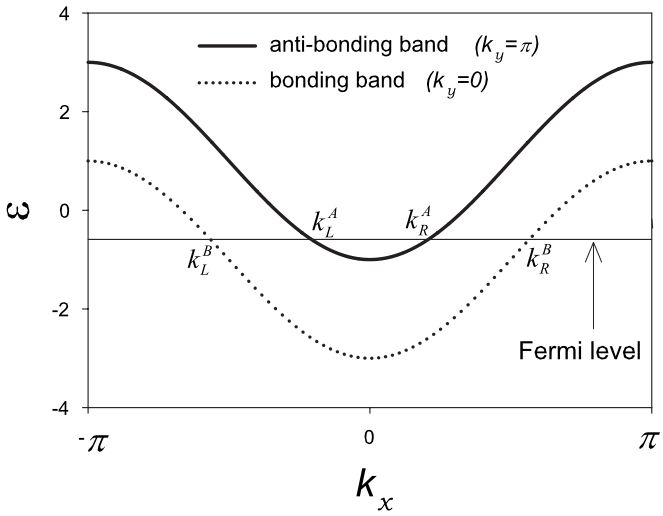

FIG. 2. Energy dispersion for free electrons in a two-leg ladder.

$$S = \int_{\underline{k},\sigma}\psi^{\dagger}_{\sigma}(\underline{k})[i\omega-\epsilon(k)]\psi_{\sigma}(\underline{k}) + \int_{\{\underline{k}\},\sigma,\sigma'} g(\underline{k}_1,\underline{k}_2,\underline{k}_3,\underline{k}_4)\psi^{\dagger}_{\sigma}(\underline{k}_4)\psi^{\dagger}_{\sigma'}(\underline{k}_3)\psi_{\sigma'}(\underline{k}_2)\psi_{\sigma}(\underline{k}_1), \quad (3)$$

where ψ is the electron field, and the coupling functions for electron-electron interactions in the momentum space are given by

$$g(\underline{k}_1,\underline{k}_2,\underline{k}_3,\underline{k}_4) = U - 2g^2_{\text{ep}}\omega_0/[\omega_0^2+(\omega_1-\omega_4)^2], \quad (4)$$

where $\underline{k}=(k,\omega)$. Each coupling is a function of the incoming and outgoing momenta and frequencies, subject to $\underline{k}_1+\underline{k}_2=\underline{k}_3+\underline{k}_4$. In order to lighten the notation, we suppress the fourth index of the coupling, showing it explicitly to emphasize the momentum or frequency dependences only. Thus, $g(\underline{k}_1,\underline{k}_2,\underline{k}_3,\underline{k}_4)$ is understood to be equivalent to $g(\underline{k}_1,\underline{k}_2,\underline{k}_3)$ with the fourth index, $\underline{k}_4$, given by $\underline{k}_4=\underline{k}_1+\underline{k}_2-\underline{k}_3$. For a system with e-ph interactions, the couplings are frequency dependent, i.e., retarded. We choose $g(\underline{k}_1,\underline{k}_2,\underline{k}_3,\underline{k}_4)$ to represent the scattering between electrons with opposite spins. The coupling functions for scattering between electrons with parallel spins are determined by those with opposite spin due to the SU(2) spin symmetry.

Following Ref. 5, our only assumption is that the full bandwidth of the two-leg ladder system is larger than any of the interaction terms; i.e., that $6t \gg U, g_{\text{ep}}, \omega_0$, leaving the relative values of U, ω_0, and g_{ep} free. The strong-coupling limit of the electron-phonon problem occurs when $\lambda \equiv 2N(0)g^2_{\text{ep}}/\omega_0 \gg 1$. This regime is accessible in our FRG approach. By utilizing the time-reversal symmetry, exchange symmetry, and reflection symmetry, the number of independent couplings in the Fermi surface for the two-leg ladder at incommensurate fillings is 12 (each coupling is a function of

three momenta and three frequencies; the frequency dependences are suppressed for clarity). There are six intraband couplings:

$$g_4^A = g(k_L^A, k_L^A, k_L^A, k_L^A), \quad g_4^B = g(k_L^B, k_L^B, k_L^B, k_L^B),$$

$$g_1^A = g(k_L^A, k_R^A, k_L^A, k_R^A), \quad g_1^B = g(k_L^B, k_R^B, k_L^B, k_R^B),$$

$$g_2^A = g(k_L^A, k_R^A, k_R^A, k_L^A), \quad g_2^B = g(k_L^B, k_R^B, k_R^B, k_L^B), \tag{5}$$

and six interband couplings:

$$g_1^C = g(k_L^A, k_L^B, k_L^A, k_L^B), \quad g_2^C = g(k_L^A, k_L^B, k_L^B, k_L^A),$$

$$g_1^D = g(k_L^B, k_R^B, k_L^A, k_R^A), \quad g_2^D = g(k_L^B, k_R^B, k_R^A, k_L^A),$$

$$g_1^E = g(k_L^B, k_R^A, k_L^B, k_R^A), \quad g_2^E = g(k_L^B, k_R^A, k_R^A, k_L^B). \tag{6}$$

III. MULTISCALE FUNCTIONAL RENORMALIZATION-GROUP METHOD

For pure e-e interactions, the Fermi velocities are renormalized by g_4^A and g_4^B, and the renormalizations of scattering between particles on the same side of the Brillouin zone at different bands, g_1^C and g_2^C, are absent in the leading order. This is not necessarily valid for couplings with frequency dependence. Moreover, these couplings generate self-energy corrections, which are important for studying the system with retardation effects,[5] leading to the renormalization of Fermi velocities and quasiparticle lifetime. Thus we keep these couplings even though they are not renormalized in the nonretarded system. In leading order, the RG equations for the coupling function, $g_\Lambda(\underline{k}_1, \underline{k}_2, \underline{k}_3)$, is

$$\partial_\Lambda g_\Lambda(\underline{k}_1, \underline{k}_2, \underline{k}_3) = -\int d\underline{p}\, \partial_\Lambda [G_\Lambda(\underline{p}) G_\Lambda(\underline{k})] g_\Lambda(\underline{k}_1, \underline{k}_2, \underline{k}) g_\Lambda(\underline{p}, \underline{k}, \underline{k}_3) - \int d\underline{p}\, \partial_\Lambda [G_\Lambda(\underline{p}) G_\Lambda(\underline{q}_1)] g_\Lambda(\underline{p}, \underline{k}_2, \underline{q}_1) g_\Lambda(\underline{k}_1, \underline{q}_1, \underline{k}_3)$$

$$- \int d\underline{p}\, \partial_\Lambda [G_\Lambda(\underline{p}) G_\Lambda(\underline{q}_2)][-2 g_\Lambda(\underline{k}_1, \underline{p}, \underline{q}_2) g_\Lambda(\underline{q}_2, \underline{k}_2, \underline{k}_3) + g_\Lambda(\underline{p}, \underline{k}_1, \underline{q}_2) g_\Lambda(\underline{q}_2, \underline{k}_2, \underline{k}_3) + g_\Lambda(\underline{k}_1, \underline{p}, \underline{q}_2) g_\Lambda(\underline{k}_2, \underline{q}_2, \underline{k}_3)]. \tag{7}$$

The RG equations for the self-energy, $\Sigma_\Lambda(\underline{k})$, is

$$\partial_\Lambda \Sigma_\Lambda(\underline{k}) = -\int d\underline{p}\, \partial_\Lambda [G_\Lambda(\underline{p})][2 g_\Lambda(\underline{p}, \underline{k}, \underline{k}) - g_\Lambda(\underline{k}, \underline{p}, \underline{k})], \tag{8}$$

where $\underline{k} = k_1 + k_2 - \underline{p}$, $q_1 = \underline{p} + k_3 - k_1$, $q_2 = \underline{p} + k_3 - k_2$, $\int d\underline{p} = \int dp \Sigma_\omega 1/(2\pi\beta)$, and G_Λ is the self-energy corrected propagator at cutoff Λ. The initial condition for the coupling functions is given by Eq. (4). The self-energies are equal to zero at $\Lambda = \Lambda_0$.

Once we obtain the renormalized couplings and self-energies, we calculate the RG flow of the susceptibilities corresponding to different order parameters and determine which one dominates. The SC susceptibility, $\chi^\delta(k, \omega)$, is defined as

$$\chi_\Lambda^\delta(k = 0, \omega = 0) = \int D(1,2) f^\delta(p_1) f^\delta(p_2) \times \langle c_{p_1,\downarrow} c_{-p_1,\uparrow} c^\dagger_{-p_2,\uparrow} c^\dagger_{p_2,\downarrow} \rangle, \tag{9}$$

where $\delta = s, d$ for s- and d-wave SC states, respectively. The form factor f^δ is defined as $f^s(p) = 1$ for s-wave SC state, and $f^d(p) = \cos(p_x) - \cos(p_y)$ for d-wave SC state. $D(1,2)$ is defined as the integration over the energy modes with energy, $|\epsilon(p_1)|$ and $|\epsilon(p_2)|$, larger than the cutoff Λ. That is, $\int D(1,2) \equiv \int_{|\epsilon(p_1)|>\Lambda} d\epsilon_1 J(\epsilon(p_1), p_1) \int_{|\epsilon(p_2)|>\Lambda} d\epsilon_2 J(\epsilon(p_2), p_2)$, where $J(\epsilon(p), p)$ is the Jacobian for the change of the integration measure from $\int dp$ to $\int d\epsilon$.

The RG equations for the susceptibility flows are

$$\partial_\Lambda \chi_\Lambda^\delta(k = 0, \omega = 0) = \int d\underline{p}\, \partial_\Lambda [G_\Lambda(\underline{p}) G_\Lambda(-\underline{p})][Z_\Lambda^\delta(\underline{p})]^2. \tag{10}$$

The function $Z_\Lambda^\delta(\underline{p})$ is the effective vertex in the definition for the susceptibility χ_Λ^δ, and its flow is governed by the RG equations:

$$\partial_\Lambda Z_\Lambda^\delta(\underline{p}) = -\int d\underline{p}'\, \partial_\Lambda [G_\Lambda(\underline{p}') G_\Lambda(-\underline{p}')] \times Z_\Lambda^\delta(\underline{p}') g_\Lambda(\underline{p}', -\underline{p}', -\underline{p}, \underline{p}). \tag{11}$$

Its initial condition, at $\Lambda = \Lambda_0$, is 1 for s-wave pairing and $\cos(k_x) - \cos(k_y)$ for d-wave pairing. The RG equations for susceptibilities are solved with initial condition $\chi^\delta_{\Lambda=\Lambda_0}(0,0) = 0$. The dominant instability in the ground state is given by the most divergent susceptibility by solving the RG equations numerically. In the calculations reported here, we have discretized the frequency axis into nine points and have checked that our results are essentially unchanged when additional discretization points are added.

IV. PAIRING SYMMETRY CHANGE DRIVEN BY ELECTRON-PHONON COUPLING

Without e-ph coupling, the *d*-wave pairing is the generic dominant instability for 0–0.5 doping (half- to quarter-filling), except in a narrow region in the parameter space where all the charge and spin degrees of freedom are gapless. The large region of *d*-wave pairing in the ladder comes from the anisotropy between the transverse and parallel directions, which leads the pair scattering to develop a directional dependence when the high-energy degrees of freedom are eliminated. For the Holstein coupling, the phonon-mediated attractive retarded interaction is independent of the momentum transfer and is thus isotropic. The attractive interaction is relevant in generating pair scattering, since it leads the particle-particle ladder diagrams to acquire logarithmic divergences. The *d*-wave pairing from repulsive interaction does not come from this divergence, and thus, the attractive interaction is very effective in leading to pairing instability, and more importantly, this pairing has *s*-wave symmetry. Therefore, the e-ph coupling tends to enhance the *s*-wave component in the pairing scattering matrix, and once this coupling exceeds a critical value, the *s*-wave channel dominates. This result can only be seen in strong coupling and, hence, is not accessible to the two-step RG.[4] A study of the fully retarded problem for a 2D circular Fermi surface has similarly shown how the two-step RG breaks down in the strong-coupling ($\lambda \gg 1$) limit.[19] Another consequence of e-ph coupling is that retardation leads to corrections to the quasiparticle lifetime. These come from self-energy corrections which depend on the density of states (i.e., on the Fermi velocity). Near half-filling the Fermi velocities of the two bands are similar. However, close to quarter-filling they are very different, the self-energy corrections are then different for the two bands, and therefore *d*-wave tendency is further enhanced when there is retardation (Fig. 1).

In Fig. 3 we show a representative RG flow, in which we observe the change in the dominant susceptibility for increasing e-ph coupling g_{ep}. Although the isotropic phonons tend to break the *d*-wave pairs, as long as the e-ph coupling is small compared to the e-e interactions, the *d*-wave pairing remains the dominant instability. However, the *s*-wave overcomes the *d*-wave pairing when the effective interaction in the antiadiabatic limit, $U_{\text{effective}}=U-2g_{ep}^2/\omega_0$, is near zero. When retardation effects are fully taken into account, the transition to *s* wave happens at a smaller value of g_{ep} than for the antiadiabatic limit. This is because the phonons have a finite energy ω_0, and at this energy scale, it is enough that the attractive part of the interaction overcomes the *renormalized* repulsive part at that RG scale in order for the *s*-wave instability to occur. As the doping increases, the critical values for the pairing transition remains constant. As quarter-filling is approached, the *d*-wave SC region then *increases* with doping and is rather stable against *s* wave, because the Fermi surface becomes more anisotropic. This result should be contrasted with the 2D case where *d*-wave SC region seems to be suppressed at larger doping because the Fermi surface becomes more isotropic. Hence, our results show that one has to be cautious when comparing results for ladders with the true 2D problem. For doping close to the quarter filling,

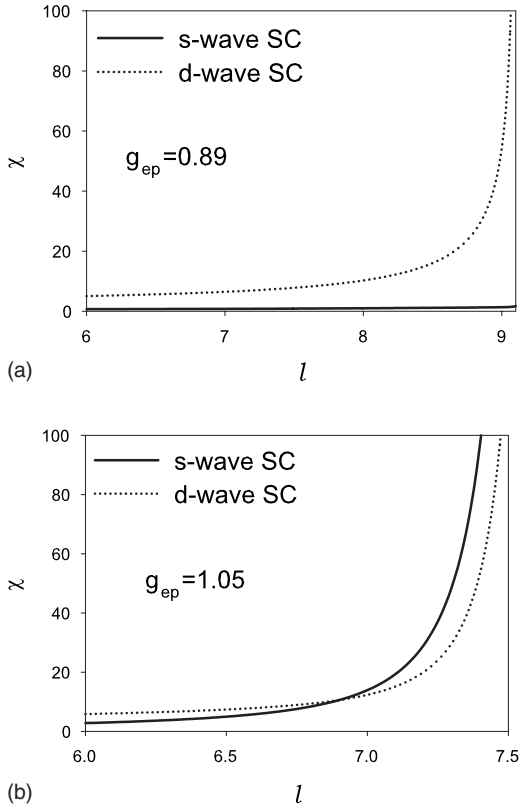

FIG. 3. The flows of *s*-wave SC (solid lines) and *d*-wave SC (dotted lines) susceptibilities as a function of $l=\ln(\Lambda_0/\Lambda)$ for $U=2$, $\omega_0=1$, and doping of 0.2.

we find noticeable changes in the critical values, and a substantially stronger e-ph interaction is needed to drive the *s*-wave pairing over the *d* wave. This can be understood from the fact that the difference between the Fermi velocities of the antibonding and bonding bands becomes larger as the system is doped away from half-filling (see Fig. 2), and from the different self-energy corrections, as discussed before. The asymmetry between the bands leads to different contributions to pair scattering at $k_y=0$ and at $k_y=\pi$, leading to a phase difference in the pairing matrix elements which is manifested as a *d*-wave pairing channel. At sufficiently strong e-ph coupling, *s* wave still dominates

Exactly at quarter-filling, the Fermi surface in the antibonding band shrinks to a point, which leads to a Van Hove singularity. Also, at this filling the distance between the Fermi points in the bonding band is commensurate, which results in the presence of an extra umklapp scattering in the bonding band, $g_3^B=(k_L^B,k_L^B,k_R^B,k_R^B)$. We do not find that the umklapp scattering is sufficient to drive the system to spin-density wave (SDW) phase. In contrast to the case without phonons, $\lambda=0$,[14] we do not find a Luttinger liquid phase (C2S2). The *d*-wave pairing is still the dominant instability for small e-ph coupling, and the *s* wave again overcomes the *d* wave at strong coupling. Below quarter-filling, the antibonding band is empty. Only two Fermi points remain on the bonding band. The system becomes essentially 1D as the effect of the antibonding band is then irrelevant.

We have also investigated the problem exactly at half-filling. In this particular commensurate doping, there is a direct competition between a SDW and a CDW phase. In the absence of e-ph interaction, the SDW phase (with a charge gap but no spin gap) is very robust and is not destabilized at weak coupling. At intermediate coupling ($\lambda \approx 1$), however, the SDW phase becomes unstable to a CDW phase with a charge gap. This result cannot be obtained in the weak-coupling methods discussed previously.

The final results of our study are summarized in the phase diagram of Fig. 1. We find that the e-ph couplings at intermediate and strong couplings leads to substantial qualitative differences from previous results, including the appearance of new phases: CDW and *s*-wave SC state. Moreover, we see that the *d*-wave phase is stabilized close to quarter-filling, in contrast to the 2D case.

V. CONCLUSION

In conclusion, we have studied the effect of e-ph coupling on the phase diagram of a two-leg ladder Holstein-Hubbard model and applied the FRG method. This method deals with the retardation effects in a systematic way. In particular, when the e-ph interaction strength is comparable to the e-e interactions and $\lambda \gg 1$, there are qualitative differences in the phase diagram from that predicted in previous studies. In particular, in addition to the SDW and *d*-wave SC phases found previously, we establish that for strong e-ph coupling, both CDW and *s*-wave SC phases can arise.

ACKNOWLEDGMENT

A.H.C.N. was supported through NSF Grant No. DMR-0343790.

[1] R. Shankar, Rev. Mod. Phys. **66**, 129 (1994).
[2] Famous counterexamples to this rule include the class of impurity problems such as the Kondo problem, in which the bulk degrees can be integrated out exactly, leading to nonperturbative results for the *boundary* degrees of freedom. See, for instance, K. G. Wilson, Rev. Mod. Phys. **47**, 773 (1975).
[3] G. T. Zimanyi, S. A. Kivelson, and A. Luther, Phys. Rev. Lett. **60**, 2089 (1998).
[4] A. Seidel, Hsiu-Hau Lin, and Dung-Hai Lee, Phys. Rev. B **71**, 220501(R) (2005).
[5] S.-W. Tsai, A. H. Castro Neto, R. Shankar, and D. K. Campbell, Phys. Rev. B **72**, 054531 (2005).
[6] J. Sólyom, Adv. Phys. **28**, 201 (1979).
[7] J. Voit, Rep. Prog. Phys. **58**, 977 (1995).
[8] K.-M. Tam, S. W. Tsai, and D. K. Campbell, Phys. Rev. Lett. **96**, 036408 (2006).
[9] J. Voit and H. J. Schulz, Phys. Rev. B **34**, 7429 (1986); **37**, 10068 (1988).
[10] D. Zanchi and H. J. Schulz, Phys. Rev. B **54**, 9509 (1996); **61**, 13609 (2000).
[11] C. J. Halboth and W. Metzner, Phys. Rev. B **61**, 7364 (2000).
[12] L. G. Caron and C. Bourbonnais, Phys. Rev. B **29**, 4230 (1984).
[13] S. R. White and D. J. Scalapino, Phys. Rev. Lett. **80**, 1272 (1998); **81**, 3227 (1998).
[14] L. Balents and M. P. A. Fisher, Phys. Rev. B **53**, 12133 (1996); H.-H. Lin, L. Balents, and M. P. A. Fisher, *ibid.* **56**, 6569 (1997).
[15] See, for instance, E. Dagotto and T. M. Rice, Science **271**, 618 (1996), and references therein.
[16] A. Lanzara, P. V. Bogdanov, X. J. Zhou, S. A. Kellar, D. L. Feng, E. D. Lu, T. Yoshida, H. Eisaki, A. Fujimori, K. Kishio, J. I. Shimoyama, T. Noda, S. Uchida, Z. Hussain, and Z. X. Shen, Nature (London) **412**, 510 (2001).
[17] Z.-X. Shen, A. Lanzara, S. Ishihara, and N. Nagaosa, Philos. Mag. B **82**, 1349 (2002).
[18] T. Ishiguro and K. Yamaji, *Organic Superconductors* (Springer-Verlag, Berlin, 1990).
[19] S.-W. Tsai, A. H. Castro Neto, R. Shankar, and D. K. Campbell, Philos. Mag. **86**, 2631 (2006).